LWT - Food Science and Technology 134 (2020) 110247

Contents lists available at ScienceDirect

LWT

journal homepage: www.elsevier.com/locate/lwt

Halloysite nanotubes as a carrier of cornelian cherry (*Cornus mas* L.) bioactives

Bojana Blagojević [a,*], Dragana Četojević-Simin [b], Filippo Parisi [c], Giuseppe Lazzara [c], Boris M. Popović [a]

[a] Department of Field and Vegetable Crops, Faculty of Agriculture, University of Novi Sad, Trg Dositeja Obradovića 8, 21000, Novi Sad, Serbia
[b] Oncology Institute of Vojvodina, Dr Goldmana 4, 21204, Sremska Kamenica, Serbia
[c] Dipartimento di Fisica e Chimica, Università Degli Studi di Palermo, Viale Delle Scienze, Pad. 17, Palermo, 90128, Italy

ARTICLE INFO

Keywords:
Halloysite
Cornelian cherry
Iridoids
Anthocyanins
Bioactivity

ABSTRACT

Cornelian cherry fruit extract rich in anthocyanins and iridoids was encapsulated in the halloysite nanotubes in order to obtain a stable nanoscale system for better delivery and prolonged release of bioactive constituents. The cyclic vacuum technique was used for halloysite nanotubes-cornelian cherry composite preparation and the loading of 8.5 wt% was achieved. Pure cornelian cherry extract exhibited antiproliferative effect on HT-29, MCF7, and MRC-5 cells, pristine halloysite nanotubes affected the growth of MCF7 cells, while halloysite nanotubes-cornelian cherry composites demonstrated proliferative activity in all tested cells. The sustained release of anthocyanins was achieved by this encapsulation strategy. Additional implementation of halloysite nanotubes-cornelian cherry into yogurt prolonged the release of iridoid molecules. Obtained results indicate that halloysite nanoclay is a suitable nanocarrier for cornelian cherry constituents that can be utilized in food and pharmaceutical industries.

1. Introduction

Halloysite is naturally occurring nanoclay, with chemical formula $Al_2SiO_5(OH)_4 \cdot nH_2O$ (Lvov & Abdullayev, 2013). It has been known for more than a hundred years and it was used for ceramics. At the beginning of the 21st century, its intensive usage has been started, especially for medicinal purposes, cosmetics, agriculture, catalysis, etc. (Churchman, Pasbakhsh, & Hillier, 2016; Sadjadi, 2020; Yuan, Tan, & Annabi-Bergaya, 2015).

A wide range of its usage, halloysite owes to its structure. The most usual halloysite form is elongated tube usually 1 μm long and approximately 50 nm wide outer diameter and 15 nm inner lumen diameter (Lvov, Aerov, & Fakhrullin, 2014). It should be noted that the characteristic sizes are highly dependent on the deposit (Cavallaro, Chiappisi, Pasbakhsh, Gradzielski, & Lazzara, 2018; Pasbakhsh, Churchman, & Keeling, 2013). The silica layer is on the outer surface and it is negatively charged (−30 mV), while the alumina layer is on the inner surface providing positive charge (+25 mV). This charge difference allows the binding of different molecules in the lumen and on the outer surface area.

Nanoscale systems of delivery of bioactive compounds represent a novel technology approach for improved bioavailability and bioactivity, predominantly because of controlled and sustained delivery management. Halloysite nanotubes (HNT) became a promising nanocarrier for bioactive compounds. Its biocompatibility and non-toxicity were confirmed in several studies, justifying its usage in biological investigations (Fakhrullina, Akhatova, Lvov, & Fakhrullin, 2015; Lai et al., 2013; Lvov, DeVilliers, & Fakhrullin, 2016; Naumenko, Guryanov, Yendluri, Lvov, & Fakhrullin, 2016; Vergaro et al., 2010). Pristine and functionalized HNT were shown to be a good system for entrapping secondary biomolecules, such as curcumin (Riela et al., 2014) and resveratrol (Vergaro, Lvov, & Leporatti, 2012).

Cornelian cherry (*Cornus mas* L.) fruit has high bioactive potential, but it is underused not sufficiently investigated. Cornelian cherry (CC) fruit is an abundant source of bioactive molecules, especially of polyphenols and iridoids (Kucharska, Szumny, Sokół-Letowska, Piórecki, & Klymenko, 2015). CC fruit constituents are proved to manifest beneficial health effects, such as antidiabetic (Dzydzan, Bila, Kucharska, Brodyak,

* Corresponding author.
E-mail addresses: bojana.blagojevic@polj.uns.ac.rs (B. Blagojević), ddaaggeerr@gmail.com (D. Četojević-Simin), filippo.parisi@unipa.it (F. Parisi), giuseppe.lazzara@unipa.it (G. Lazzara), boris.popovic@polj.uns.ac.rs (B.M. Popović).

https://doi.org/10.1016/j.lwt.2020.110247
Received 15 June 2020; Received in revised form 9 September 2020; Accepted 16 September 2020
Available online 19 September 2020

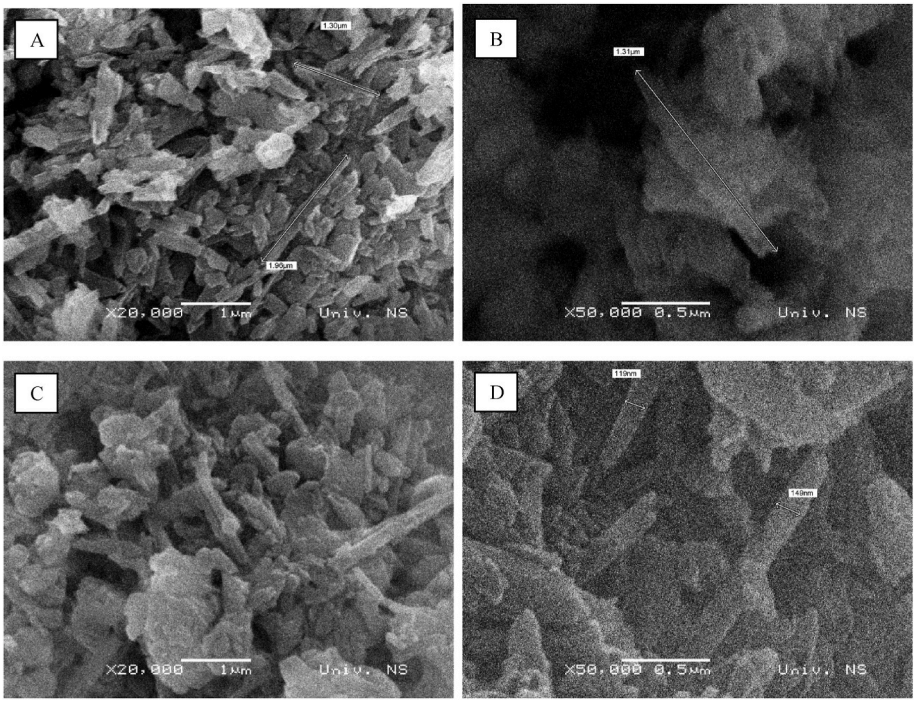

Fig. 1. SEM micrographs of pristine halloysite (HNT; A, B) and halloysite-cornelian cherry (HNT-CC) encapsulates (C, D) performed with different magnifications (20,000x and 50,000x).

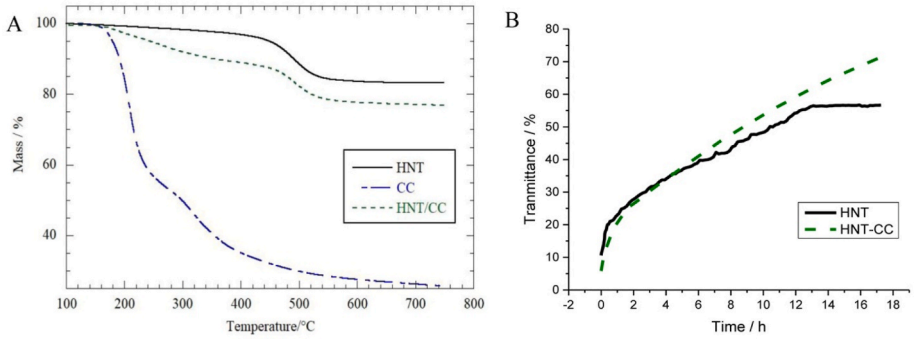

Fig. 2. Thermogravimetric curves (A) and transmittance at 800 nm as a function of time (B) for the investigated samplesAbbreviations: CC – cornelian cherry fruit extract, HNT – halloysite nanotubes, HNT-CC – halloysite-cornelian cherry encapsulate.

& Sybirna, 2019), antilipidemic (Sozański et al., 2014), immunomodulatory (Piekarska, Szczypka, Kucharska, & Gorczykowski, 2018), and antiinflammatory (Sozański et al., 2016).

In this research, for the first time HNT was used and assessed as a carrier for the CC fruit extract. The aim was to obtain efficiently loaded and stable composite that would provide better bioavailability and controlled release of CC bioactives. Considering food fortification with natural resources as one of the very useful strategies to improve bioaccessibility of nutrients and bioactive compounds (Gahruie, Eskandari, Mesbahi, & Hanifpour (2015), food ingredients, such as fruits, are often added to yogurt (Trigueros, Pérez-Alvarez, Viuda-Martos, & Sendra, 2011). In our study, yogurt was enriched with the obtained halloysite-cornelian cherry encapsulate in order to increase yogurt nutritional functionality and to examine the effect on controlled release kinetics of cornelian cherry bioactives.

2. Materials and methods

All reagents and materials were used as purchased (Aldrich), without further purification. For cell tests were used human cell lines MCF7 (breast adenocarcinoma, ECACC No. 86012803), HT-29 (colon adenocarcinoma, ECACC No. 91072201), and MRC-5 (human fetal lung, ECACC No. 84101801), Dulbecco's modified Eagle's medium (DMEM; PAA Laboratories GmbH, Pashing, Austria), fetal calf serum (FCS; PAA Laboratories GmbH, Pashing, Austria), penicillin and streptomycin (Galenika, Belgrade, Serbia), trypsin (from porcine pancreas, 60 U/mg; Serva, Heidelberg, Germany).

Halloysite used in this study was the Matauri Bay halloysite from Northland, New Zealand, supplied by Imerys Tableware, New Zealand. Halloysite nanotubes from this deposit vary in length up to 2 μm, inner diameter 15–70 nm, outer diameter 50–200 nm, and wall thickness 20–200 nm. Particles are dominantly long and thin or short and stubby, tubular, with cylindrical pore shape (Pasbakhsh et al., 2013).

2.1. Fruit extracts

Cornelian cherry fruits (*Cornus mas* L.) of the Svetlyachok cultivar were harvested in September 2017, from the orchard of the Faculty of Agriculture University of Novi Sad, at Rimski Šančevi, Serbia. The stones were removed by hand and stoneless fresh fruits were frozen at −70 °C

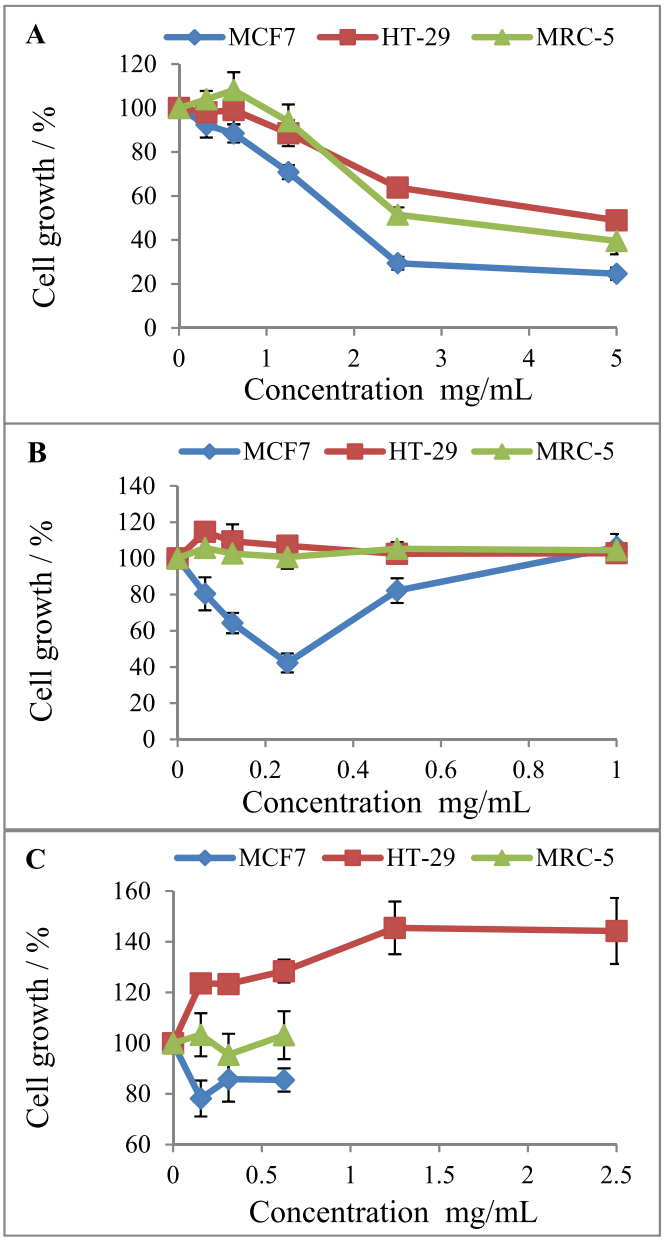

Fig. 3. CC extract (A), pristine HNT (B), and HNT-CC encapsulate (C) effects on the cell growth of MCF7, HT-29, and MRC-5 cell lines.
Abbreviations: CC – cornelian cherry, HNT – halloysite nanotubes, HNT-CC – halloysite-cornelian cherry encapsulate, MCF7 – breast adenocarcinoma cells, HT-29 – colon adenocarcinoma cells, MRC-5 – normal fetal lung fibroblasts.

overnight afterward they were lyophilized (Alpha 1–2 LDplus freeze dryer, Martin Christ, Osterode am Harz, Germany). Lyophilized fruits were ground into powder. The extraction procedure was performed by the method of Popović et al., 2020. Extracts were prepared by 20 min ultrasound extraction of 20 g of lyophilized fruits with 400 mL of 50% ethanol-water (v/v) as a solvent. The mixture was additionally stirred at 600 rpm for 2 h in the dark. After centrifugation (9500×*g*, 10 min) supernatant was filtered. Part of the extract was evaporated to dryness to obtain the mass of the dry extract for further calculation of the extract volume that should be added for the appropriate ratio of the core and coating material for the encapsulation.

2.2. Loading procedure

Halloysite nanotubes (10 g), as a dry powder, was mixed with the appropriate volume of the ethanol-water fruit extract containing 2 g of dry extract in order to obtain the 1:5 core to carrier mass ratio. The encapsulation of the organic substances within the halloysite cavity was performed by aqueous suspensions using a vacuum pumping strategy to enhance the loading efficacy as described previously (Lisuzzo, Cavallaro, Pasbakhsh, Milioto, & Lazzara, 2019).

2.3. Physico-chemical characterization

Halloysite nanotubes and cornelian cherry encapsulates were recorded by scanning electron microscope (SEM, JEOL JSM 6460 LV, Tokyo, Japan) operating at 20 kV.

The thermogravimetric analyses (TGA) were carried out by using a Q5000 IR apparatus (TA Instruments) under nitrogen flow (25 cm^3/min) at the heating rate of 20 °C/min to 750 °C. Before the heating ramp, the samples were equilibrated at 100 °C for 1 h to remove adsorbed water. The amount of organic material entrapped into the HNT was estimated from the thermogravimetric curves by taking into account the residual mass at 750 °C.

The stability of the encapsulates was assessed by measuring the transmittance of the HNT and HNT-CC particles dispersed in the solution at 25 °C during the time, using a UV–Vis spectrophotometer (Specord S 600, Analytik Jena AG) (Cavallaro, Lazzara, Milioto, & Parisi, 2016). The sedimentation experiment was monitored at a wavelength of 800 nm, at which no absorbance bands were detected and the results were expressed as the percentage of transmittance.

2.4. Antiproliferative activity

2.4.1. Cells

Human cell lines MCF7 (breast adenocarcinoma), HT-29 (colon adenocarcinoma), and MRC-5 (fetal lung fibroblasts) were used for the evaluation of the antiproliferative activity. Cell lines were grown in Dulbecco's modified Eagle's medium (DMEM) with 45 mg/mL glucose, supplemented with 10% heat-inactivated fetal calf serum (FCS), 100 IU/mL of penicillin and 100 μg/mL of streptomycin. They were cultured in 25 cm^2 flasks at 37 °C in an atmosphere of 5% CO_2, high humidity and subcultured twice a week. Single-cell suspension was obtained using 100 mg/100 mL trypsin with 40 mg/100 mL EDTA (Četojević-Simin et al., 2015).

2.4.2. Samples used in the antiproliferative assay

Samples were dissolved and diluted in DMSO to obtain the required final concentrations. The final concentrations were in the range from 60 to 5000 μg/mL, whereas the final concentration of DMSO in the samples was ≤0.05% (v/v).

2.4.3. SRB test

Cell lines were harvested and plated into 96-well microtiter plates at the seeding density of 4–8 x 10^3 cells per well, in a volume of 199 μL, and preincubated in complete medium supplemented with 5% FCS, at 37 °C for 24 h. Serial dilutions of samples or solvent (1 μL per well) were added to the test and control wells, respectively. Microplates were then incubated at 37 °C for an additional 48 h. Cell growth was evaluated by the modified (Četojević-Simin et al., 2004) colorimetric Sulforhodamine B (SRB) assay according to (Skehan et al., 1990). Cells were fixed with 50% TCA (1 h, 4 °C), washed with distilled water and stained with 0.4% SRB (30 min, room temperature). The plates were then washed with 1% acetic acid to remove the unbound dye. Protein-bound dye was extracted with 10 mmol/L Tris base. Absorbance was measured on a microplate reader (Multiscan Ascent, Labsystems) at 540/620 nm. The effect on cell growth was calculated by Eq. (1):

$$\text{Cell growth } (\%) = \frac{A_{sample}}{A_{control}} \times 100\ (\%) \quad (1)$$

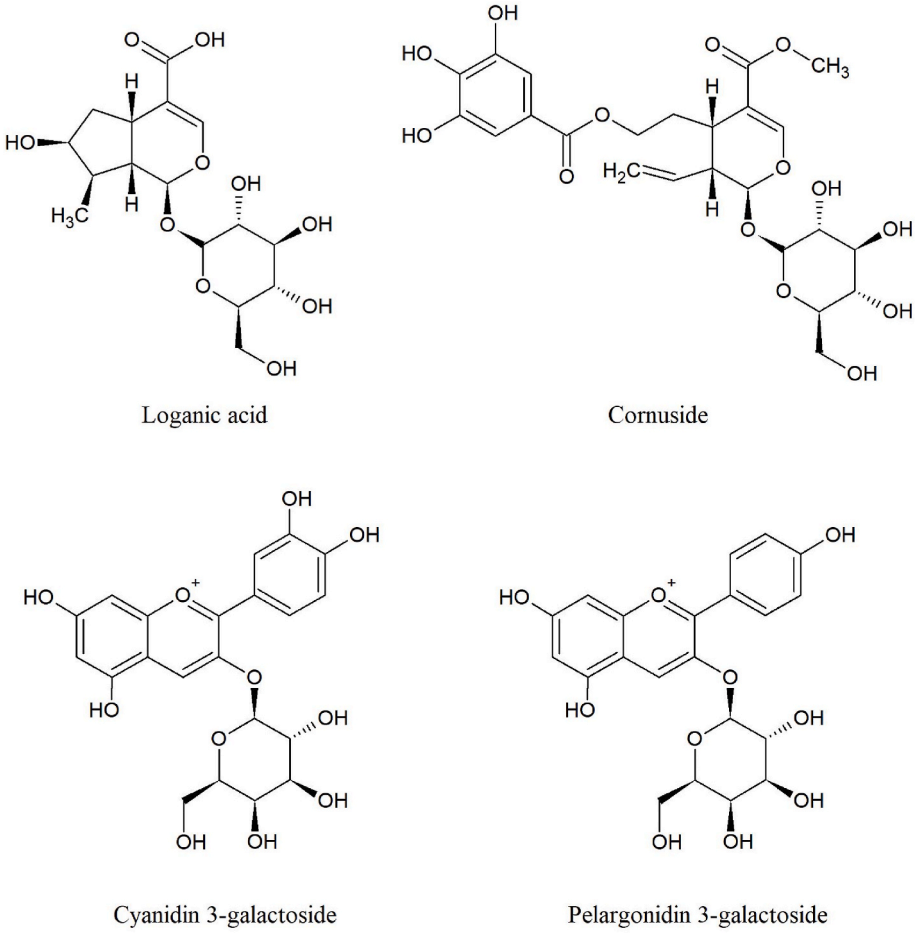

Fig. 4. Chemical structures of cornelian cherry (*Cornus mas* L.) most dominant bioactive constituents.

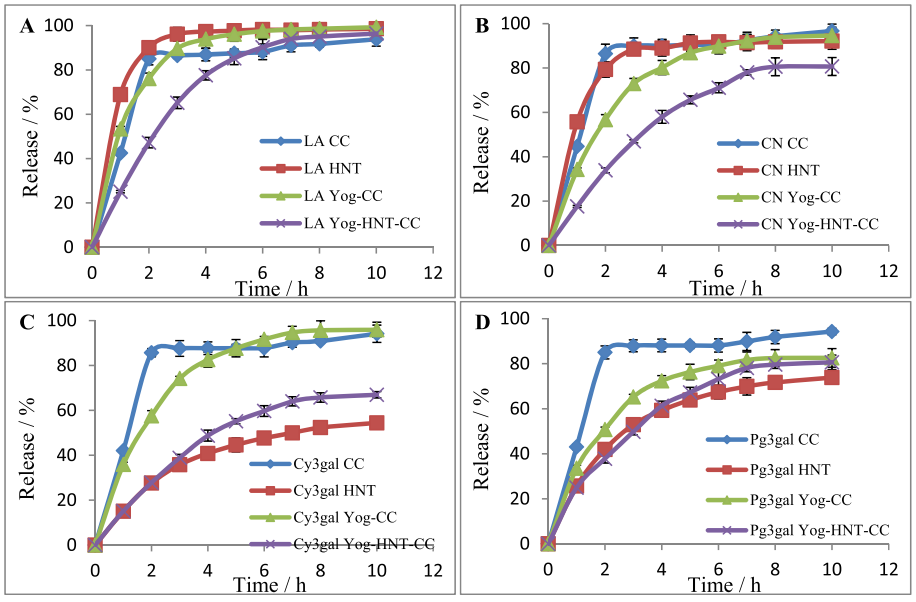

Fig. 5. Controlled release of cornelian cherry bioactive constituents from fruit extract, halloysite encapsulate and in combination with yogurt: (A) Loganic acid – LA; (B) Cornuside – CN; (C) Cyanidin 3-galactoside – Cy3gal; (D) Pelargonidin 3-galactoside – Pg3gal.
Abbreviations: CC – cornelian cherry fruit extract, HNT – halloysite nanotubes, Yog – yogurt, Yog-CC – yogurt enriched with cornelian cherry fruit extract, Yog-HNT-CC – yogurt enriched with halloysite-cornelian cherry encapsulate.

where A_{sample} and $A_{control}$ were the absorbances of the test sample and negative control.

2.5. Yogurt fortification with CC extract and HNT-CC encapsulate

Plain yoghurt was obtained from a local supermarket. By the producer declaration, it contains 2.8 g of fat, 4.2 g of carbohydrates, and 3.1 g of proteins on 100 g. The yogurt was enriched with fruit extract

and with HNT-CC encapsulates in 1:0.5 and 1:3 ratio, based on the lyophilized mass of plain yogurt. Final mixtures were lyophilized for further controlled release analysis (Ghorbanzade, Jafari, Akhavan, & Hadavi, 2017).

2.6. Controlled release kinetics

For the release kinetics study, 0.5 g of the encapsulate was placed in the molecular porous membrane, with 6–8 kD molecular weight cut off (MWCO; Spectra/Por, Spectrum Laboratories, Inc., CA, USA). On both ends, the membrane was closed with weighted closures and submerged into 25 mL of distilled water pH 7.4. It was stirred at 60 rpm and 37 °C. Each hour, part of the release medium was taken out for HPLC analysis and replaced with the same volume of water to maintain the volume. The total amounts of bioactive compounds released were calculated by Eq. (2):

$$Cn' = Cn + \frac{V}{V_0} \times \sum_{i=0}^{n-1} Ci \quad (2)$$

where *Cn'* is corrected concentration, *Cn* is *n*th concentration, *V* is the volume of the sample withdrawn for each analysis, *Vo* is the total volume, and *Ci* is the concentration at the time i (i < n) (Lisuzzo, Cavallaro, Milioto, & Lazzara, 2019).

For the estimation of total compound content present in the sample, the samples were extracted with the system for the total bioactive compounds described in section 2.8.

2.7. HPLC-PDA analysis of phenolic and iridoid CC profile

Compounds were identified by the method of (Popović et al., 2020), using Shimadzu Nexera X2 HPLC system (Tokyo, Japan), equipped with a photodiode array (PDA) detector. Compounds were separated at 40 °C on Luna C18 (2), 3 μm, 2 × 150 mm column, with a C18 guard column, 2 × 4 mm (Phenomenex, Torrance, CA, USA). Binary gradient was used for elution, combining 1% formic acid in water (solvent A) and 1% formic acid in methanol (solvent B) as follows: 0–10 min, 5–20% B; 10–13 min, 20% B; 13–30 min, 20–25% B; 30–35 min, 25–30% B; 35–45 min, 30–70% B; 45–50 min, 70% B; 50–55 min, 70–100% B; 55–65 min, 100% B; 65–75 min, 100-5% B; and 5 min post run time. The flow rate was 0.25 mL/min, and the injection volume was 3 μL. UV–vis absorption spectra were recorded in the wavelength range of 190–650 nm, with ref. wavelength/bandwidth 620/20 nm. Chromatograms were plotted at wavelengths: 245 nm (iridoids), 254 nm (ellagic acid), 320 nm (hydroxycinnamic acids), 350 nm (flavonols), and 520 nm (anthocyanins).

2.8. Spectrophotometric encapsulation efficiency assessment

The experiment was performed on the basis of the method described by (Saénz, Tapia, Chávez, & Robert, 2009). For the extraction of total bioactive compounds (TBC), 100 mg of sample was dispersed in 1 mL ethanol:acetic acid:water (50:8:42, v/v/v), vortexed for 1 min and ultrasonicated twice for 20 min. For the surface bioactive compounds (SBC) extraction, 100 mg of sample was dispersed in 1 mL of ethanol: methanol (50:50, v/v) and vortexed for 1 min. The mixtures were then centrifuged at 9500×*g* for 5 min, filtered through 0.45 μm sized syringe filters and subjected to further analysis.

Bioactive compounds were determined by Folin-Ciocalteau method (Ainsworth & Gillespie, 2007), mixing 200 μL of the sample with 1 mL of the 0.1 mol/L FC reagent and the addition of 800 μL of 7.5 g/100 mL Na_2CO_3. The absorbance was read after 60 min at the wavelength of 760 nm using Thermo Scientific Evolution 220 UV–vis spectrophotometer. The results were calculated by the calibration curve prepared with the gallic acid. The encapsulation efficiency (EE) was determined as the ratio of core to total bioactive compounds, where the core bioactive compounds are presented as subtraction of SBC from TBC (Eq. (3)):

$$EE\ (\%) = \frac{TBC - SBC}{TBC} \times 100\ (\%) \quad (3)$$

2.9. Statistical analysis

All the measurements were performed in triplicates and the results were expressed as the mean value ± standard deviation (SD). The data were analyzed using Statistica 13.3 software (TIBCO Software Inc, Palo Alto, CA, USA). Statistical comparison between the samples of controlled release analysis was done by one-way analysis of variance (ANOVA) with Duncan's multiple range tests for independent observations ($P < 0.01$).

3. Results and discussion

3.1. Physico-chemical characterization

The surface morphology of the pure HNT and HNT-CC encapsulates was imaged by SEM (Fig. 1). It could be seen the tendency of HNT to polydisperse in length (Pasbakhsh et al., 2013). This tendency is also noticed after combining with the fruit extract. The shape of the HNT was maintained in HNT-CC encapsulates, but the nanotubes were more glued together.

Halloysite nanotubes showed the typical thermogram of the nanoclay with a mass loss of 16.3 wt% related to the volatilization of the interlayer water molecules at ca. 500 °C (Fig. 2A). The cornelian cherry extracts had a degradation with a two steps mechanism occurring at 210 °C and 320 °C. The loaded HNT showed a decrease of residual mass at high temperature because the organic moiety thermally decomposes in the range from 150 to 350 °C. As concerns the mass loss profile, the loaded halloysite clearly evidenced the features of the pristine components indicating the successful loading of the CC into the HNT. From the quantitative analysis of the mass losses, one can estimate that the loading efficiency is 8.5 wt% that is consistent with the full loading of the cavity based on the HNT typical sizes (Cavallaro et al., 2018).

The colloidal stability of the pristine HNT and HNT-CC was assessed by the turbidity measurement of the solutions in which particles were dispersed. It was monitored by the transmittance as a function of the time. The data presented in Fig. 2B show that HNT-CC particles are less stable than the pristine HNT. The presence of CC extract made bigger aggregates in the solution, which caused faster sedimentation of the particles. CC fruit extracts contain high amounts of organic compounds, like sugars, vitamins, organic acids that could be wrapped around the nanotubes causing their stickiness and glued them together (Martinović & Cavoski, 2020; Yilmaz, Ercisli, Zengin, Sengul, & Kafkas, 2009). For the first 6 h, HNT and HNT-CC were equally stable, to the transmittance of 40%. Afterward, the HNT-CC sedimentation proceeded continuously. In the case of pristine HNT after reaching around 60% of transmittance in the 12th hour, it stayed constant.

3.2. Antiproliferative activity

Previous work (Vergaro et al., 2010) proved the biocompatibility of the HNT and showed that nanotubes enter the cells. In this study, the antiproliferative activities of CC extract, pristine HNT, and HNT-CC encapsulate were assessed in human breast adenocarcinoma cells MCF7, human colon adenocarcinoma cells HT-29, and normal fetal lung fibroblasts MRC-5. The results were presented in Fig. 3. In all three cell lines, CC dry extract exhibited growth inhibition in a dose-dependent manner. The IC_{50} values were 1712.87 ± 143.93, 4204.14 ± 530.71, and 2541.07 ± 162.89 μg/mL for MCF7, HT-29, and MRC-5 cells, respectively. The growth of HT-29 and MRC-5 cells was maintained at the control level under the exposure to pristine NHT. HNT affected the growth of MCF7 cells. The results indicated that HNT concentrations

inhibited growth of MCF7 cells in a dose-dependent manner, and with $IC_{50} = 137.09 \pm 7.64$ μg/mL. These results are in agreement with those of Vergaro et al. (2010).

Non-cytotoxic and even proliferative effects were observed for HNT-CC treatment (Fig. 3C). In HT-29 cells stimulation of cell growth was observed in all concentrations. In MCF7 and MRC-5 cells, at higher concentrations (>1000 μg/mL) interference with the SRB test was observed, so the results and IC_{50} value could not be accurately determined. In these cell lines at lower encapsulate concentrations cellular growth was at the level of controls. Within HNT-CC treatment, the concentrations of the CC extract that were delivered to the cells were much lower compared with examined pure CC extract that expressed inhibitory effects, i.e. low doses of CC bioactives delivered by HNT affected cell growth by increase of cell proliferation.

3.3. HPLC-PDA analysis of bioactive compounds of cornelian cherry fruits and release kinetics

CC fruits are abundant in iridoid molecules and polyphenols, among which anthocyanins predominate (Kucharska et al., 2015). Iridoid and phenolic profiles of the CC extract obtained by HPLC-PDA analysis are shown in Table S1. Loganic acid is the major iridoid compound present in CC extract, followed by the cornuside content. Among anthocyanins, cyanidin 3-galactoside and pelargonidin 3-galactoside were the most dominant. These four molecules together constituted *ca.* 94% of all detected iridoid and phenolic compounds and were monitored in the controlled release study. Their structures are presented in Fig. 4.

The results presented in Fig. 5 (A and B), Table S3, and Table S4 showed that encapsulation with HNT did not affect the release of iridoid molecules and they were totally released after the second hour. However, when HNT-CC was implemented to yogurt, the release of loganic acid and cornuside was significantly prolonged. These results suggest that yoghurt proteins additionally interact with the tubes affecting the release of bioactive constituents.

On the other side, encapsulation with HNT significantly affected the release of anthocyanin molecules (Fig. 5C and D; Table S5; Table S6). Because of the positive charge of the anthocyanin molecules, they are more likely bound predominantly on the negative outer surface area of the HNT. Compared with cyanidin 3-galactoside, the higher percentage of pelargonidin 3-galactoside was released, indicating the influence of the structure on binding to the tubes. Cyanidin has the additional –OH group on B ring of the flavonoid structure (Fig. 4), which can provide tighter binding by the additional hydrogen bond or through chelating with the aluminium ion on the inner surface area of HNT (Kumar & Pandey, 2013). Almost the same release trend of anthocyanins was preserved after the implementation of encapsulates into the yogurt.

Encapsulation efficiency obtained by the spectrophotometric method was 35.87% for the HNT-CC encapsulate, and 61.42 and 20.93% after yogurt fortification with pure CC extract and HNT-CC encapsulates, respectively (Table S2).

It was shown that yogurt proteins (whey proteins and caseins) are suitable wall material for the encapsulation and controlled delivery of the anthocyanins and other phenolics from fruit extracts (Norkaew, Thitisut, Mahatheeranont, & Pawin, 2019; Ouyang et al., 2020). Other investigations confirmed very good loading of proteins into the halloysite tubes, or on their outer surface area, depending on the protein charge (Lvov et al., 2014). Our results provide the basis for further investigations of functionalized HNT for more prolonged release and targeted delivery of CC constituents.

4. Conclusion

Results obtained in this study proved the possibility of HNT to be used as a nanocarrier for the CC bioactive constituents. Efficiently loaded encapsulates with the impact on cell proliferation and sustained release of cyanidin 3-galactoside and pelargonidin 3-galactoside, two major anthocyanins in CC fruits were obtained. Additional fortification of yogurt with HNT-CC encapsulates provided the gradual release of iridoid molecules, too. Obtained composites were promoted as functional food ingredients and supplements. Considering immense health benefits that CC constituents possess, further composite functionalization should be investigated for improved release and targeted delivery of bioactive polyphenolic and iridoid compounds, and possible usage in the pharmaceutical industry.

CRediT authorship contribution statement

Bojana Blagojević: Formal analysis, Investigation, Data curation, Writing - original draft. **Dragana Četojević-Simin:** Formal analysis, Investigation, Validation, Resources, Writing - review & editing. **Filippo Parisi:** Investigation, Data curation. **Giuseppe Lazzara:** Resources, Validation, Formal analysis, Writing - review & editing. **Boris M. Popović:** Conceptualization, Methodology, Validation, Resources, Writing - review & editing, Supervision, Funding acquisition.

Declaration of competing interest

The authors declare that they have no known competing financial interests or personal relationships that could have appeared to influence the work reported in this paper.

Acknowledgement

This research was financially supported by the Ministry of Education, Science and Technological Development, Republic of Serbia, Contract No. 451-03-68/2020-14/200117 and the Provincial Secretariat for Sports and Youth of the Autonomous Province of Vojvodina.

Appendix A. Supplementary data

Supplementary data to this article can be found online at https://doi.org/10.1016/j.lwt.2020.110247.

References

Ainsworth, E. A., & Gillespie, K. M. (2007). Estimation of total phenolic content and other oxidation substrates in plant tissues using Folin-Ciocalteu reagent. *Nature Protocols, 2*(4), 875–877. https://doi.org/10.1038/nprot.2007.102

Cavallaro, G., Chiappisi, L., Pasbakhsh, P., Gradzielski, M., & Lazzara, G. (2018). A structural comparison of halloysite nanotubes of different origin by Small-Angle Neutron Scattering (SANS) and Electric Birefringence. *Applied Clay Science, 160*, 71–80. https://doi.org/10.1016/j.clay.2017.12.044. August 2017.

Cavallaro, G., Lazzara, G., Milioto, S., & Parisi, F. (2016). Steric stabilization of modified nanoclays triggered by temperature. *Journal of Colloid and Interface Science, 461*, 346–351. https://doi.org/10.1016/j.jcis.2015.09.046

Četojević-Simin, D. D., Čanadanović-Brunet, J. M., Bogdanović, G. M., Ćetković, G. S., Tumbas, V. T., & Djilas, S. M. (2004). Antioxidative and antiproliferative effects of Satureja Montana L. extracts. *Journal of BUON, 9*, 443–449.

Četojević-Simin, D. D., Velićanski, A. S., Cvetković, D. D., Markov, S. L., Ćetković, G. S., Tumbas Šaponjac, V. T., et al. (2015). Bioactivity of Meeker and Willamette raspberry (*Rubus idaeus* L.) pomace extracts. *Food Chemistry, 166*, 407–413. https://doi.org/10.1016/j.foodchem.2014.06.063

Churchman, G. J., Pasbakhsh, P., & Hillier, S. (2016). The rise and rise of halloysite. *Clay Minerals, 51*(3), 303–308. https://doi.org/10.1180/claymin.2016.051.3.00

Dzydzan, O., Bila, I., Kucharska, A. Z., Brodyak, I., & Sybirna, N. (2019). Antidiabetic effects of extracts of red and yellow fruits of cornelian cherries (*Cornus mas* L.) on rats with streptozotocin-induced diabetes mellitus. *Food & Function, 10*(10), 6459–6472. https://doi.org/10.1039/c9fo00515c

Fakhrullina, G. I., Akhatova, F. S., Lvov, Y. M., & Fakhrullin, R. F. (2015). Toxicity of halloysite clay nanotubes in vivo: A Caenorhabditis elegans study. *Environmental Sciences: Nano, 2*(1), 54–59. https://doi.org/10.1039/c4en00135d

Gahruie, H. H., Eskandari, M. H., Mesbahi, G., & Hanifpour, M. A. (2015). Scientific and technical aspects of yogurt fortification: A review. *Food Science and Human Wellness, 4*(1), 1–8. https://doi.org/10.1016/j.fshw.2015.03.002

Ghorbanzade, T., Jafari, S. M., Akhavan, S., & Hadavi, R. (2017). Nano-encapsulation of fish oil in nano-liposomes and its application in fortification of yogurt. *Food Chemistry, 216*, 146–152. https://doi.org/10.1016/j.foodchem.2016.08.022

Kucharska, A. Z., Szumny, A., Sokół-Letowska, A., Piórecki, N., & Klymenko, S. V. (2015). Iridoids and anthocyanins in cornelian cherry (*Cornus mas* L.) cultivars. *Journal of*

Food Composition and Analysis, 40, 95–102. https://doi.org/10.1016/j.jfca.2014.12.016

Kumar, S., & Pandey, A. K. (2013). *Chemistry and biological activities of Flavonoids : An overview*, 2013.

Lai, X., Agarwal, M., Lvov, Y. M., Pachpande, C., Varahramyan, K., & Witzmann, F. A. (2013). Proteomic profiling of halloysite clay nanotube exposure in intestinal cell co-culture. *Journal of Applied Toxicology, 33*(11), 1316–1329. https://doi.org/10.1002/jat.2858

Lisuzzo, L., Cavallaro, G., Milioto, S., & Lazzara, G. (2019). Layered composite based on halloysite and natural polymers: A carrier for the pH controlled release of drugs. *New Journal of Chemistry, 43*(27), 10887–10893. https://doi.org/10.1039/c9nj02565k

Lisuzzo, L., Cavallaro, G., Pasbakhsh, P., Milioto, S., & Lazzara, G. (2019). Why does vacuum drive to the loading of halloysite nanotubes? The key role of water confinement. *Journal of Colloid and Interface Science, 547*, 361–369. https://doi.org/10.1016/j.jcis.2019.04.012

Lvov, Y., & Abdullayev, E. (2013). Progress in Polymer Science Functional polymer – clay nanotube composites with sustained release of chemical agents. *Progress in Polymer Science, 38*(10–11), 1690–1719. https://doi.org/10.1016/j.progpolymsci.2013.05.009

Lvov, Y., Aerov, A., & Fakhrullin, R. (2014). *Clay nanotube encapsulation for functional biocomposites* (Vol. 207, pp. 189–198). https://doi.org/10.1016/j.cis.2013.10.006

Lvov, Y. M., DeVilliers, M. M., & Fakhrullin, R. F. (2016). The application of halloysite tubule nanoclay in drug delivery. *Expert Opinion on Drug Delivery, 13*(7), 977–986. https://doi.org/10.1517/17425247.2016.1169271

Martinović, A., & Cavoski, I. (2020). The exploitation of cornelian cherry (*Cornus mas* L.) cultivars and genotypes from Montenegro as a source of natural bioactive compounds. *Food Chemistry, 318*(February), 126549. https://doi.org/10.1016/j.foodchem.2020.126549

Naumenko, E. A., Guryanov, I. D., Yendluri, R., Lvov, Y. M., & Fakhrullin, R. F. (2016). Clay nanotube-biopolymer composite scaffolds for tissue engineering. *Nanoscale, 8*(13), 7257–7271. https://doi.org/10.1039/c6nr00641h

Norkaew, O., Thitisut, P., Mahatheeranont, S., & Pawin, B. (2019). Effect of wall materials on some physicochemical properties and release characteristics of encapsulated black rice anthocyanin microcapsules. *Food Chemistry, 294*(May), 493–502. https://doi.org/10.1016/j.foodchem.2019.05.086

Ouyang, Y., Chen, L., Qian, L., Lin, X., Fan, X., & Teng, H. (2020). Fabrication of caseins nanoparticles to improve the stability of cyanidin 3-O-glucoside. *Food Chemistry, 317*(February), 126418. https://doi.org/10.1016/j.foodchem.2020.126418

Pasbakhsh, P., Churchman, G. J., & Keeling, J. L. (2013). Characterisation of properties of various halloysites relevant to their use as nanotubes and microfibre fillers. *Applied Clay Science, 74*, 47–57. https://doi.org/10.1016/j.clay.2012.06.014

Piekarska, J., Szczypka, M., Kucharska, A. Z., & Gorczykowski, M. (2018). Effects of iridoid-anthocyanin extract of *Cornus mas* L. on hematological parameters, population and proliferation of lymphocytes during experimental infection of mice with *Trichinella spiralis*. *Experimental Parasitology, 188*, 58–64. https://doi.org/10.1016/j.exppara.2018.03.012

Popović, B. M., Blagojević, B., Ždero Pavlović, R., Mićić, N., Bijelić, S., Bogdanović, B., et al. (2020). Comparison between polyphenol profile and bioactive response in blackthorn (*Prunus spinosa* L.) genotypes from north Serbia-from raw data to PCA analysis. *Food Chemistry, 302*, 125373. https://doi.org/10.1016/j.foodchem.2019.125373

Riela, S., Massaro, M., Colletti, C. G., Bommarito, A., Giordano, C., Milioto, S., et al. (2014). Development and characterization of co-loaded curcumin/triazole-halloysite systems and evaluation of their potential anticancer activity. *International Journal of Pharmaceutics, 475*(1), 613–623. https://doi.org/10.1016/j.ijpharm.2014.09.019

Sadjadi, S. (2020). Halloysite-based hybrids/composites in catalysis. *Applied Clay Science, 189*(February), 105537. https://doi.org/10.1016/j.clay.2020.105537

Saénz, C., Tapia, S., Chávez, J., & Robert, P. (2009). Microencapsulation by spray drying of bioactive compounds from cactus pear (*Opuntia ficus-indica*). *Food Chemistry, 114*(2), 616–622. https://doi.org/10.1016/j.foodchem.2008.09.095

Skehan, P., Storeng, R., Scudiero, D., Monks, A., Mcmahon, J., Vistica, D., et al. (1990). New colorimetric cytotoxicity assay for anticancer-drug screening. *Journal of the National Cancer Institute, 82*(13), 1107–1112. https://doi.org/10.1093/jnci/82.13.1107

Sozański, T., Kucharska, A. Z., Rapak, A., Szumny, D., Trocha, M., Merwid-Ląd, A., et al. (2016). Iridoid–loganic acid versus anthocyanins from the *Cornus mas* fruits (cornelian cherry): Common and different effects on diet-induced atherosclerosis, PPARs expression and inflammation. *Atherosclerosis, 254*, 151–160. https://doi.org/10.1016/j.atherosclerosis.2016.10.001

Sozański, T., Kucharska, A. Z., Szumny, A., Magdalan, J., Bielska, K., Merwid-Ląd, A., et al. (2014). The protective effect of the *Cornus mas* fruits (cornelian cherry) on hypertriglyceridemia and atherosclerosis through PPARα activation in hypercholesterolemic rabbits. *Phytomedicine, 21*, 1774–1784. https://doi.org/10.1016/j.phymed.2014.09.005

Trigueros, L., Pérez-Alvarez, J. A., Viuda-Martos, M., & Sendra, E. (2011). Production of low-fat yogurt with quince (*Cydonia oblonga* Mill.) scalding water. *LWT – Food Science and Technoogy, 44*(6), 1388–1395.

Vergaro, V., Abdullayev, E., Lvov, Y. M., Zeitoun, A., Cingolani, R., Rinaldi, R., et al. (2010). Cytocompatibility and uptake of halloysite clay nanotubes. *Biomacromolecules, 11*(3), 820–826. https://doi.org/10.1021/bm9014446

Vergaro, V., Lvov, Y. M., & Leporatti, S. (2012). Halloysite clay nanotubes for resveratrol delivery to cancer cells. *Macromolecular Bioscience, 12*(9), 1265–1271. https://doi.org/10.1002/mabi.201200121

Yilmaz, K. U., Ercisli, S., Zengin, Y., Sengul, M., & Kafkas, E. Y. (2009). Preliminary characterisation of cornelian cherry (*Cornus mas* L.) genotypes for their physico-chemical properties. *Food Chemistry, 114*(2), 408–412. https://doi.org/10.1016/j.foodchem.2008.09.055

Yuan, P., Tan, D., & Annabi-Bergaya, F. (2015). Properties and applications of halloysite nanotubes: Recent research advances and future prospects. *Applied Clay Science, 112*(113), 75–93. https://doi.org/10.1016/j.clay.2015.05.001